Microscopic nuclear equation of state with three-body forces and neutron star structure

M. Baldo, G.F. Burgio

Dipartimento di Fisica, Universitá di Catania and I.N.F.N. Sezione di Catania, c.so Italia 57, I-95129 Catania, Italy

and I. Bombaci

Dipartimento di Fisica, Universitá di Pisa and I.N.F.N. Sezione di Pisa, Piazza Torricelli 2,

I-56100 Pisa, Italy

Abstract

We calculate static properties of non-rotating neutron stars (NS's) using a microscopic equation of state (EOS) for asymmetric nuclear matter. The EOS is computed in the framework of the Brueckner–Bethe–Goldstone many–body theory. We introduce three-body forces in order to reproduce the correct saturation point of nuclear matter. A microscopic well behaved EOS is derived. We obtain a maximum mass configuration with $M_{max} = 1.8M_{\odot}$, a radius R = 9.7 km and a central density $n_c = 1.34 \ fm^{-3}$. We find the proton fraction exceeds the critical value x^{Urca} , for the onset of direct Urca processes, at densities $n \ge 0.45 \ fm^{-3}$. Therefore, in our model, NS's with masses above $M^{Urca} = 0.96M_{\odot}$ can undergo very rapid cooling depending on whether or not nucleon superfluidity in the interior of the NS takes place. A comparison with other microscopic models for the EOS is done, and neutron star structure is calculated for these models too.

PACS numbers: 97.60.Jd, 21.65.+f

In the next few years it is expected that a large amount of novel informations on neutron stars (NS's) will be available from the new generation of X-ray and γ -ray satellites. Therefore, a great interest is devoted presently to the study of NS's and to the prediction of their structure on the basis of the properties of dense matter. The equation of state (EOS) of NS matter covers a wide density range, from $\sim 10 \text{ g/cm}^3$ in the surface to several times nuclear matter saturation density ($\rho_0 \sim 2.8 \ 10^{14} \ {\rm g/cm^3}$) in the center of the star [1]. The interior part (core) of a NS is made by asymmetric nuclear matter with a certain lepton fraction. At ultra-high density, matter might suffer a transition to other exotic hadronic components (like hyperons, a K^- condensate or a deconfined phase of quark matter). The possible appearance of such an exotic core has enormous consequences for the neutron star and black hole formation mechanism [2]. Unfortunately large uncertainities are still present in the theoretical treatment of this ultra-dense regime [3,4]. Therefore, in the present work, we consider a more conventional picture assuming the NS core is composed only by an uncharged mixture of neutrons, protons, electrons and muons in equilibrium with respect to the weak interaction (β -stable matter). Even in this picture, the determination of the EOS of asymmetric nuclear matter to describe the core of the NS, remains a formidable theoretical problem [5].

Any "realistic" EOS must satisfy several requirements : i) It must display the correct saturation point for symmetric nuclear matter (SNM); ii) it must give a symmetry energy compatible with nuclear phenomenology and well behaved at high densities; iii) for SNM the incompressibility at saturation must be compatible with phenomenology on monopole nuclear oscillations [6]; iv) both for neutron matter (NEM) and SNM the speed of sound must not exceed the speed of light (causality condition), at least up to the relevant densities; the latter condition is automatically satisfied only in fully relativistic theory.

In this letter we present results for some NS properties obtained on the basis of a microscopic EOS, recently developed [7], which satisfies requirements i-iv, and compare them with the predictions of other microscopic EOS's. The Brueckner-Hartree-Fock (BHF) approximation for the EOS in SNM, within the continuous choice [8], reproduces closely the

Brueckner–Bethe–Goldstone (BBG) results which include up to four hole line diagram contributions |9|, as well as the variational calculations |10|, at least up to few times the saturation density. Non-relativistic calculations, based on purely two-body interactions, fail to reproduce the correct saturation point for SNM. This well known deficiency is commonly corrected introducing three-body forces (TBF). Unfortunately, it seems not possible to reproduce the experimental binding energies of light nuclei and the correct saturation point accurately with one simple set of TBF [10]. Relevant progress has been made in the theory of nucleon TBF, but a complete theory is not yet available. In ref. [10] a set of simple TBF has been introduced within the variational approach. We introduced [7] similar TBF within the BHF approach, and we have adjusted the parameters in order to reproduce closely the correct saturation point of SNM, since for NS studies this is an essential requirement, and there is no reason to believe that TBF be the same as in light nuclei. The corresponding EOS (termed BHF3) is depicted in Fig. 1, in comparison with the EOS obtained in BHF approximation without three-body forces (BHF2), but using the same two-body force, i.e. the Argonne v_{14} (Av_{14}) potential [11]). In the same figure, we show the variational EOS (WFF) of ref. [10] for the $Av_{14} + TBF$ Hamiltonian, and the EOS from a recent Dirac-Brueckner calculation (DBHF) [12] with the Bonn–A two–body force. The BHF3 EOS saturates at $n_o = 0.18 \ fm^{-3}, E = -15.88 \ MeV$, and is characterized by an incompressibility $K_{\infty} = 240 \ MeV$, very close to the recent phenomenological estimate of ref. [6]. In the low density region ($n < 0.4 \ fm^{-3}$), BHF3 and DBHF equations of state are very similar. At higher density, however, the DBHF is stiffer than the BHF3. The discrepancy between these two models for the EOS can be easily understood by noticing that the DBHF treatment is equivalent [13] to introduce in the non-relativistic BHF2 the three-body force corresponding to the excitation of a nucleon-antinucleon pair, the so-called Z-diagram [14]. The latter is repulsive at all densities. In BHF3 treatment, on the contrary, both attractive and repulsive three-body forces are introduced [10], and therefore a softer EOS can be expected.

Fractional polynomial fits to each one of these EOS's allow to compute the corresponding pressure and speed of sound c_s to compare with the speed of light c. The ratio c_s/c for all four

EOS's as a function of the number density is reported in Fig. 2. WFF model (circles) violates the causality condition at densities encountered in the core of stars near the maximum mass configuration for that model (see fig. 4b) and tab. I). The DBHF calculations need an extrapolation to slightly higher densities than the largest one considered in ref. [12]. The extrapolation was done in such a way to keep the causality condition fulfilled. The same procedure was followed for BHF3. In the latter case the BHF procedure was well converging up to densities $n = 0.76 \ fm^{-3}$ for SNM and $n = 0.912 \ fm^{-3}$ for NEM. For DBHF the causality condition was fulfilled in the extrapolated region only if particular choices of the fitting parameters were used, while for the BHF3 the results were insensitive to a wide range of variation of the parameters [15].

It has to be stressed that the β -stable matter EOS is strongly dependent on the nuclear symmetry energy, which in turns affects the proton concentration [16]. The latter quantity is crucial for the onset of direct Urca processes [17], whose occurrence enhances neutron star cooling rates. In our approach, from the difference of the energy per particle E/A in NEM and SNM the symmetry energy E_{sym} can be extracted assuming a parabolic dependence on the asymmetry parameter $\beta = (n_n - n_p)/(n_n + n_p)$, being n_n and n_p respectively the neutron and proton number density. This procedure turns out to be quite reliable [16]. The values of E_{sym} for the different EOS's are reported in Fig. 3, together with the corresponding proton fraction $x = (1 - \beta)/2$. We notice that in both relativistic and non-relativistic Bruecknertype calculations, the proton fraction can exceed the "critical" value $x^{Urca} = (11 - 15)\%$ needed for the occurrence of direct Urca processes [17]. This is at variance with the WFF variational calculation (Fig. 3, circles), which predicts a low absolute value both for the simmetry energy and the proton fraction with a slight bend over. For BHF3 model we find $x^{Urca} = 13.6\%$, which correspond to a critical density $n^{Urca} = 0.447 \ fm^{-3}$. Therefore, BHF3 neutron stars with a central density higher than n^{Urca} develop inner cores in which direct Urca processes are allowed.

The EOS for β -stable matter can be used in the Tolman–Oppenheimer–Volkoff [18] equations to compute the neutron star mass and radius as a function of the central density.

For the outer part of the neutron star we have used the equations of state by Feynman-Metropolis-Teller [19] and Baym-Pethick-Sutherland [20], and for the middle-density regime $(0.001 \ fm^{-3} < n < 0.08 \ fm^{-3})$ we use the results of Negele and Vautherin [21]. In the high-density part $(n > 0.08 \ fm^{-3})$ we use alternatively the three EOS's discussed above. The results are reported in Fig. 4. We display the gravitational mass M_G , in units of solar mass M_{\odot} $(M_{\odot} = 1.99 \ 10^{33} \ g)$, as a function of the radius R (panel (a)) and the central number density n_c (panel (b)). As expected, the stiffest EOS (DBHF) we used in the present calculation gives higher maximum mass and lower central density with respect to the non-relativistic Brueckner models. The maximum NS mass for the BHF3 is intermediate between BHF2 and DBHF, but closer to the latter. The difference between BHF3 and WFF neutron stars reflects the discrepancy already noticed for the EOS and mainly for the symmetry energy. This point will be discussed in more details in a forthcoming paper [15]. Table I summarizes maximum mass configuration properties, for the different EOS's used in the present work.

In conclusion, we computed some properties of NS's on the basis of a microscopic EOS obtained in the framework of BBG many-body theory with two- and three-body nuclear interactions. BHF3 EOS satisfies the general physical requirements (points i-iv) discussed in the introduction. This is the main feature which distinguishes our BHF3 EOS with respect to other microscopic non-relativistic EOS [10,22]. The calculated maximum mass is in agreement with observed NS masses [23]. We found that the neutron star core is "proton rich". In fact, the proton fraction at the center of the maximum mass configuration in the BHF3 model is x = 26%. Our BHF3 neutron stars with mass above the critical value $M^{Urca} \equiv M_G(n^{Urca}) = 0.96M_{\odot}$ develop inner cores in which direct Urca processes can take place. These stars cool very rapidly or not depending on the properties of nuclear superluidity (values of the superfluid gaps, critical temperatures, density ranges for the superfluid transition) [24,25]. Our EOS offers the possibility for a selfconsistent microscopic calculation for both the neutron star structure, and nuclear superfluid properties within the same many-body approach and with the same nuclear interaction.

REFERENCES

- S. Shapiro and S. Teukolsky, "Black Holes, White Dwarfs and Neutron Stars", (John Wiley & Sons 1983) USA.
- [2] I. Bombaci, Astron. and Astrophys. **305**, 871 (1996)
- [3] N.K. Glendenning, Astrophys. Jour. **293**, 470 (1985)
- [4] M. Prakash, I. Bombaci, M. Prakash, P.J. Ellis, R. Knorren, J.M. Lattimer, *Phys. Rep.* (1996), (to be published).
- [5] M. Hjorth–Jensen, T.T.S. Kuo and E. Osnes, *Phys. Rep.* **261**, 125 (1995).
- [6] W.D. Myers and W.J. Swiatecky, Nucl. Phys. A601, 141 (1996).
- [7] M. Baldo and G. Giambrone, in preparation.
- [8] M. Baldo, I. Bombaci, L.S. Ferreira, G. Giansiracusa and U. Lombardo, *Phys. Rev.* C43, 2605 (1991) and references therein.
- [9] B.D. Day and R.B. Wiringa, *Phys. Rev.* C32, 1057 (1985).
- [10] R.B. Wiringa, V. Fiks and A. Fabrocini, *Phys. Rev.* C38, 1010 (1988).
- [11] R.B. Wiringa, R.A. Smith and T.L. Ainsworth, *Phys. Rev.* C29, 1207 (1984).
- [12] G.Q. Li, R. Machleidt and R. Brockmann, Phys. Rev. C45, 2782 (1992).
- [13] M. Baldo, G. Giansiracusa, U. Lombardo, I. Bombaci and L.S. Ferreira, Nucl. Phys. A583, 599 (1995).
- [14] G.E. Brown, W. Weise, G. Baym and J. Speth, Comm. Nucl. Part. Phys. 17, 39 (1987).
- [15] M. Baldo, I. Bombaci and G.F. Burgio, in preparation.
- [16] I. Bombaci and U. Lombardo, *Phys. Rev.* C44, 1892 (1991).
- [17] J. Lattimer, C. Pethick, M. Prakash and P. Haensel, Phys. Rev. Lett. 66, 2701 (1991).

- [18] R.C. Tolman, Proc. Nat. Acad. Sci. USA 20, 3 (1934); J. Oppenheimer and G. Volkoff, Phys. Rev. 55, 374 (1939).
- [19] R. Feynman, F. Metropolis and E. Teller, *Phys. Rev.* **75**, 1561 (1949).
- [20] G. Baym, C. Pethick and D. Sutherland, Astrophys. J. 170, 299 (1971).
- [21] J. W. Negele and D. Vautherin, Nucl. Phys. A207, 298 (1973).
- [22] L. Engvik, M. Hjorth-Jensen, G. Bao, E. Osnes and E. Ostgaard, Astrophys. Jour. (1996) (in press); Phys. Rev. Lett. 73, 2650 (1994).
- [23] M.H. van Kerkwijk, J. van Paradijs and E.J. Zuiderwijk, Astron. and Astrophys. 303, 497 (1995)
- [24] D. Page and J.H. Applegate, Astrophys. Jour. **394**, L17 (1992)
- [25] M. Baldo, U. Lombardo, I. Bombaci and P. Schuck, Phys. Rep. 242, 159 (1995) and references therein.

EOS	M_G/M_{\odot}	R(km)	$n_c(fm^{-3})$
DBHF	2.063	10.39	1.13
BHF3	1.794	9.74	1.34
BHF2	1.59	7.96	1.95
WFF	2.13	9.4	1.25

TABLES

TABLE I. Parameters of the maximum mass configuration: the ratio M_G/M_{\odot} is shown for several EOS's vs. the corresponding radius R and central number density n_c .

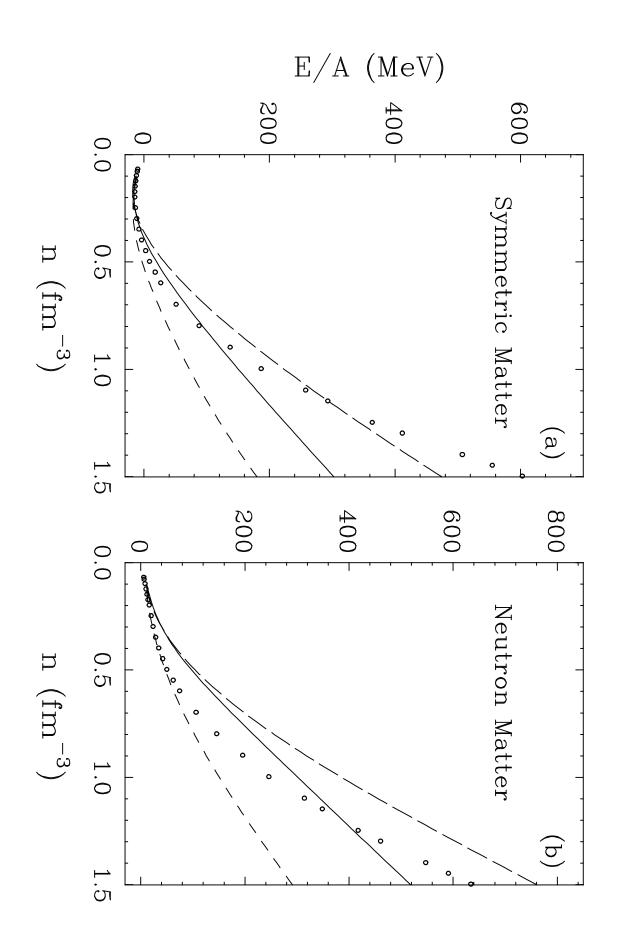
FIGURES

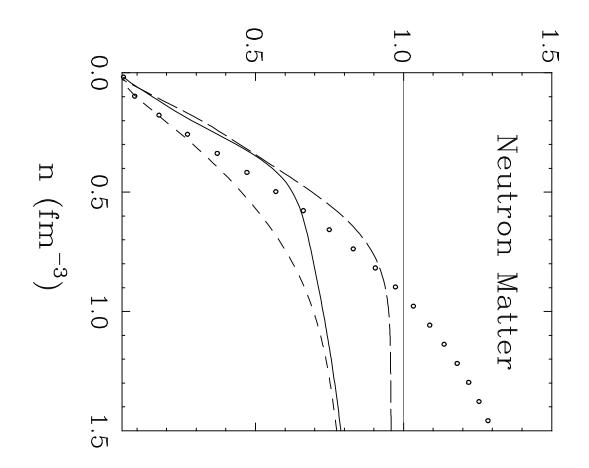
FIG. 1. The energy per baryon E/A is plotted vs. the number density n for symmetric matter (panel (a)) and for neutron matter (panel (b)). Several EOS's are shown, *i.e.* non-relativistic Brueckner calculations without (short dashes, BHF2) and with three-body forces (solid line, BHF3) and a relativistic Dirac-Brueckner one (long dashes, DBHF). For comparison a variational calculation is also reported (circles, WFF).

FIG. 2. The ratio c_s/c is plotted as a function of the number density for pure neutron matter. The different curves refer to BHF2 (short dashes), BHF3 (solid line), DBHF (long dashes) and the variational calculations of ref. [10] (circles).

FIG. 3. The simmetry energy and the proton fraction are shown vs. number density respectively in panel (a) and (b). The different curves refer to BHF2 (short dashes), BHF3 (solid line), DBHF (long dashes) and the variational calculation WFF (circles).

FIG. 4. The gravitational mass M_G , expressed in units of solar mass M_{\odot} , is displayed vs. radius R and the central number density n_c . The notation is the same as in previous figures.





 c_s/c

